Citation: Molecular Therapy — Methods & Clinical Development (2014) **1,** 8; doi:10.1038/mtm.2013.8

www.nature.com/mtm

ARTICLE

Adipose tissue insulin receptor knockdown via a new primate-derived hybrid recombinant AAV serotype

Xianglan Liu[1,2], Daniel Magee[1,2], Chuansong Wang[1,2], Travis McMurphy[1,2], Andrew Slater[1,2], Matthew During[1,2] and Lei Cao[1,2]

Adipose tissue plays an essential role in metabolic homeostasis and holds promise as an alternative depot organ in gene therapy. However, efficient methods of gene transfer into adipose tissue *in vivo* have yet to be established. Here, we assessed the transduction efficiency to fat depots by a family of novel engineered hybrid capsid serotypes (Rec1~4) recombinant adeno-associated viral (AAV) vectors in comparison with natural serotypes AAV1, AAV8, and AAV9. Rec2 serotype led to widespread transduction in both brown fat and white fat with the highest efficiency among the seven serotypes tested. As a proof-of-efficacy, Rec2 serotype was used to deliver Cre recombinase to adipose tissues of insulin receptor floxed animals. Insulin receptor knockdown led to decreased fat pad mass and morphological and molecular changes in the targeted depot. These novel hybrid AAV vectors can serve as powerful tools to genetically manipulate adipose tissue and provide valuable vehicles to gene therapy targeting adipose tissue.

Molecular Therapy — Methods & Clinical Development (2014) **1**, 8; doi:10.1038/mtm.2013.8; published online 5 February 2014

INTRODUCTION

Adipose tissue has been recognized as a multifunctional organ that plays important roles in modulating metabolic, endocrine, and immunological processes and disease pathology.[1] Approaches to genetically manipulate adipose tissue are essential to mechanistic studies of adipose function. Up to date, genetic manipulation of adipose tissue is primarily relied on transgenic mice. However, transgenic technology can be costly, time consuming, difficult to distinguish development effects from maintenance effects, and unable to apply to species other than mouse. Viral vectors can serve as an attractive alternative. Targeting adipose tissues or adipocyte in culture with adenovirus, retrovirus, and lentivirus have been investigated with various degrees of efficiency.[2,3] The limitations of these viral vectors include adverse immunogenic effects, or tropism to dividing cells. In contrast, adeno-associated viral (AAV) vectors have been extensively used for gene delivery for experimental and therapeutic purposes in a range of animal models and clinical trials.[4,5] AAVs are nonpathogenic and low immunogenic and can transduce both dividing and postmitotic tissues and generally sustain long-term transgene expression in animal models and humans. In animal models, multiple organs have been successfully and safely transduced by recombinant AAV (rAAV) vectors including liver, heart, skeletal muscle, brain, and eye.[4] However, AAV-mediated gene delivery to adipose tissue has not been extensively investigated. A few recent reports show that AAV1 vector is more efficient than AAV2, 3, 4, and 5. However, the feasible transduction requires excipients such as Pluronic F88 (ref. 6) or celastrol.[7]

In this study, we evaluated the transduction efficiency of a family of newly engineered AAV serotypes.[8] Three newly identified nonhuman primate serotypes: cy5 (cynomolgus macague-variant 5), rh20 (rhesus macaque-variant 20), and rh39 (rhesus macaque-variant 20) have shown greater transduction efficiency than rAAV8 in the brain.[9,10] To improve transduction efficiency and select desirable tropism, novel hybrid AAV capsid serotypes: Rec1, 2, 3, and 4 were generated by shuffling the fragments of capsid sequences that matched in all three nonhuman primate AAV seroptyes cy5, rh20, and rh39 and AAV8 (ref. 8). Rec2 serotype vector showed high transduction efficiency in both brown adipose tissue (BAT) and white adipose tissue (WAT) superior to all the natural serotypes tested including AAV1, AAV8, and AAV9. A proof-of-principle of this improved technology was demonstrated by the Rec2-mediated Cre-loxP knockdown of insulin receptor (IR) in adult mice.

RESULTS

Rec2 serotype transduces WAT efficiently

To evaluate the efficacy of multiple serotypes of AAV vectors targeting WAT *in vivo*, we generated pseudotyping vectors in which a transgene cassette flanked by AAV2-inverted repeats (ITR) was packaged into the capsid from another AAV serotype including three natural serotypes: AAV1, AAV8, and AAV9 as well as the four novel serotypes generated by capsid shuffling strategy: Rec1, 2, 3, and 4. Green fluorescent protein (GFP) controlled by a ubiquitous CBA promoter (hybrid cytomegalovirus–chicken β-actin) was used as the reporter. A single dose of AAV vectors (1×10^{10} vector genomes (vg) per injection) was injected to the inguinal WAT (IWAT) of 6-week-old C57BL/6 mice. Four weeks after rAAV injection, GFP expression was examined by immunohistochemistry and western blot. AAV1 and AAV9 led to minimal GFP expression (Figures 1a and 2a). All of the novel engineered serotypes resulted in marked transgene expression (Figures 1a and 2a). In particular, Rec2 showed widespread GFP expression, and transgene expression was more than twofolds higher than AAV8 (Figures 1a and 2a,b). Mizukami *et al.* reported the

[1]Department of Molecular Virology, Immunology, and Medical Genetics, The Ohio State University, Columbus, Ohio, USA; [2]The Comprehensive Cancer Center, The Ohio State University, Columbus, Ohio, USA. Correspondence: Lei Cao (lei.cao@osumc.edu)
Received 1 October 2013; accepted 15 November 2013

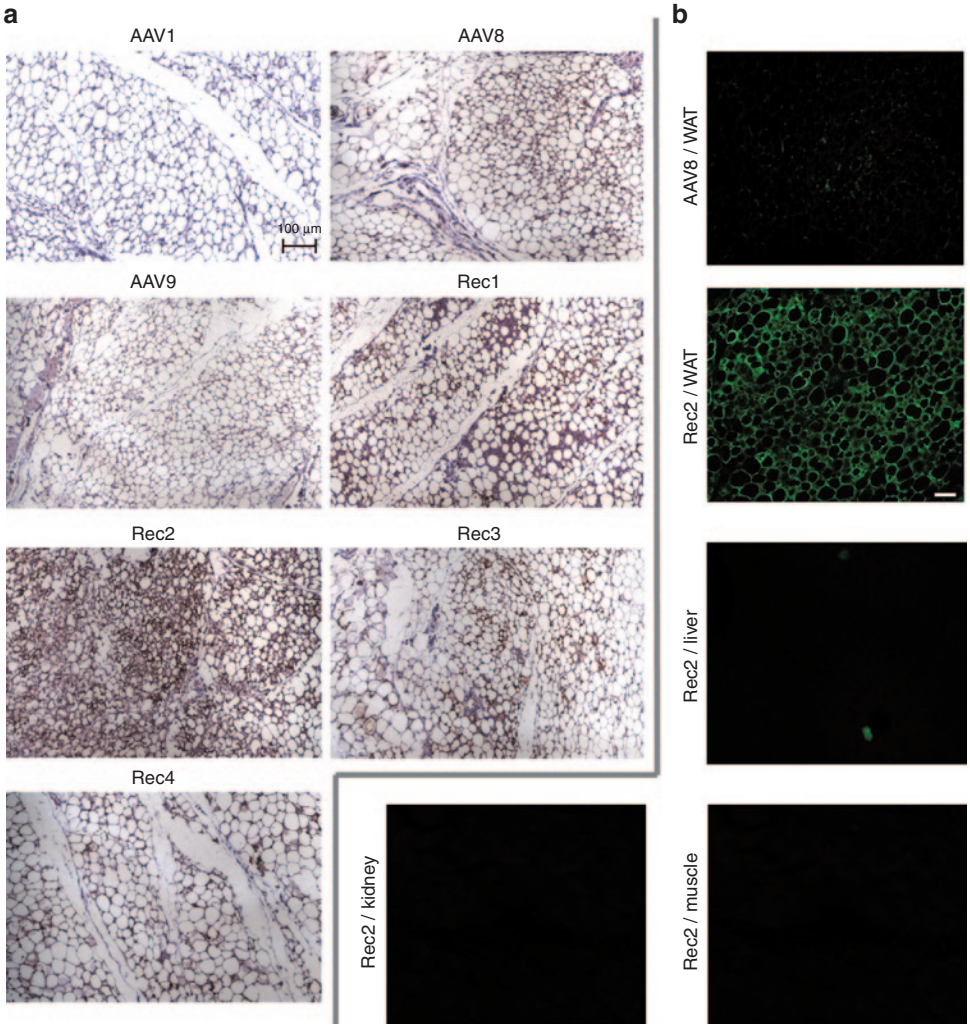

Figure 1 Comparison of transduction efficiency of novel engineered AAV serotypes with natural serotypes in white fat. (**a**) GFP immunohistochemistry of IWAT 4 weeks after rAAV injection. Scale bar = 100 μm. (**b**) GFP immunofluorescence of AAV8- and Rec2-injected IWAT (pictures were taken with the same exposure) and GFP fluorescence of liver, kidney, and skeletal muscle adjacent to IWAT. Scale bar = 50 μm. AAV, adeno-associated virus; GFP, green fluorescent protein; IWAT, inguinal white adipose tissue; rAAV, recombinant AAV.

in vivo transduction efficiency of AAV serotypes 1, 2, 3, 4, and 5. The highest transduction in IWAT was AAV1 vector in combination with Pluronic F88.[6] The dose in this study was threefold lower than that used in the study by Mizukami *et al*., and the transduction efficiency was far more superior to the rAAV1 plus Pluronic F88.[6] No transgene expression was found in nearby muscle, kidney (Figure 1b), or brain (data not shown) of Rec2-injected mice. Scarce GFP-positive cells were observed in the liver (Figure 1b) of Rec2-injected mice, while high level of GFP fluorescence was observed in liver of mice injected with AAV1, AAV8, and AAV9 (data not shown) probably because the high infection efficiency of Rec2 to the IWAT prevented the Rec2 vectors to enter the circulation.

To evaluate the transduction efficiency of Rec2 vector to visceral fat, a single dose of Rec2-GFP (1×10^{10} vg per injection) was injected to the retroperitoneal WAT. GFP fluorescence was observed 10 days after Rec2 vector injection (Figure 2c).

Rec2 serotype transduces BAT efficiently

The transduction efficacy of AAV vectors to BAT has not been examined. We assessed the gene transfer efficiency to BAT by the three natural serotypes and the four novel engineered serotypes. Preliminary data showed that Rec2 transduced BAT more efficiently than IWAT. Therefore, lower dose (1×10^9 vg per injection, bilaterally) was used in the comparison study of the seven serotypes. Similar to IWAT, AAV1 and AAV9 showed the least transgene expression (Figure 3b,c). Rec2 led to the highest transgene expression, at least twofolds of that of AAV8 (Figure 3a–c). Rec2-mediated GFP expression was widespread and more evenly distributed than that was in IWAT possibly due to bilateral injection as well as better tropism to BAT. The dose was three orders lower than that often used for systemic delivery. The low dose of Rec2 (2×10^9 vg per fat pad) was even lower than the dose we often used to transduce hypothalamus via stereotactic surgery (1×10^{10} vg per injection).[11,12] Given the much larger size of BAT compared with hypothalamus, Rec2 showed strikingly high transduction efficiency to BAT.

Rec2-Cre knocks down IR in WAT

Rec2 vector showed the highest transgene expression in both BAT and IWAT among the seven serotypes tested. In addition, Rec2 generally packages higher titer than Rec1, 3, or 4. Therefore, we chose Rec2 to demonstrate the functional efficacy of the AAV-mediated adipose gene transfer. Pseudotype Rec2 vector harboring Cre under

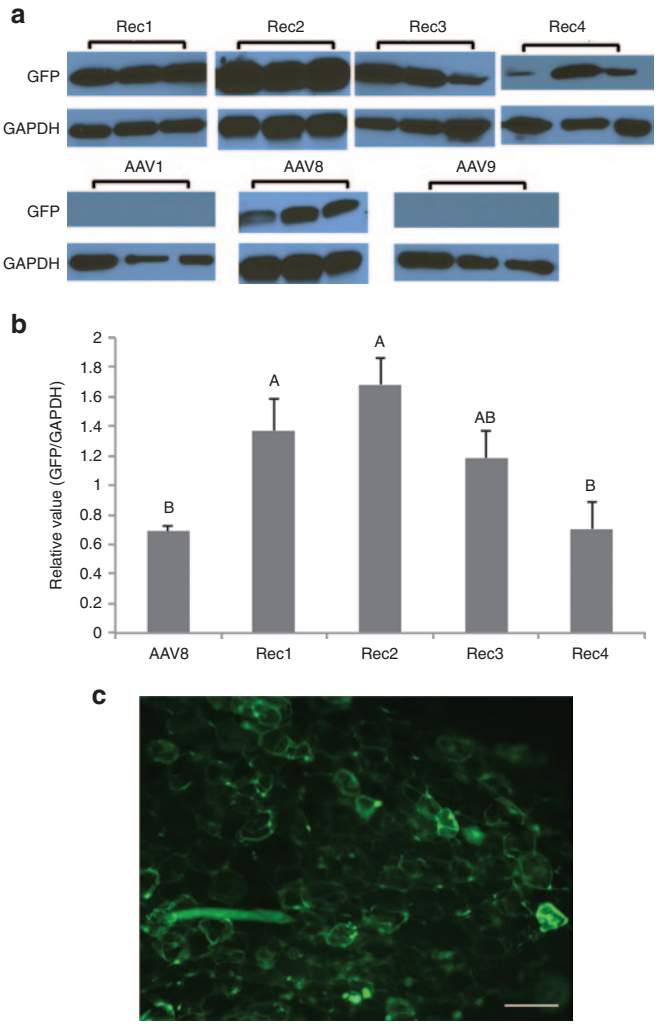

Figure 2 Quantification of transgene expression mediated by seven AAV serotypes. (**a**) Representative western blot of IWAT. (**b**) Quantification of western blot. Values are calibrated to GAPDH and expressed as mean ± SEM (n = 6 per group). Bars not connected by same letter are significantly different. (**c**) GFP fluorescence 10 days after Rec2-GFP injection to retroperitoneal WAT. Image was taken from 90 µm cryosection. Scale bar = 100 µm. AAV, adeno-associated virus; GAPDH, glyceraldehyde-3-phosphate dehydrogenase, GFP, green fluorescent protein; IWAT, inguinal WAT; WAT, white adipose tissue.

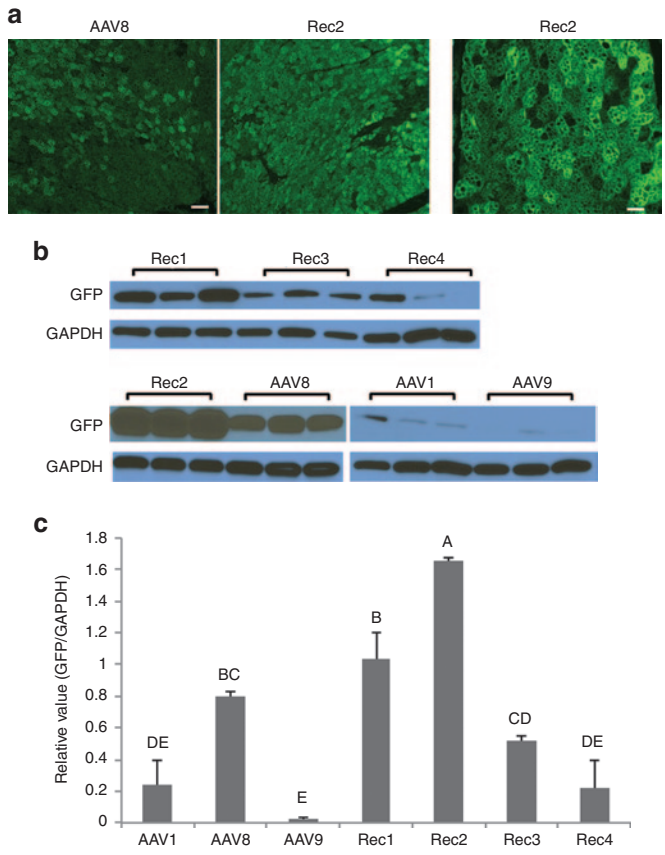

Figure 3 Comparison of transduction efficiency of novel engineered AAV serotypes with natural serotypes in brown fat. (**a**) GFP immunofluorescence of AAV8- and Rec2-injected BAT (pictures were taken with the same exposure). Scale bar = 50 µm. (**b**) Representative western blot of BAT. (**c**) Quantification of western blot. Values are calibrated to GAPDH and expressed as mean ± SEM (n = 6 per group). Bars not connected by same letter are significantly different. AAV, adeno-associated virus; BAT, brown adipose tissue; GAPDH, glyceraldehyde-3-phosphate dehydrogenase GFP, green fluorescent protein.

the control of CBA promoter was injected to both IWAT pads of 6-week-old female IR^{lox} mice (1×10^{10} vg per injection). High-level GFP expression in AAV vector–injected adipose tissue was associated with inflammation and fibrosis (data not shown). The toxicity was likely due to the transgene instead of vector itself since neither inflammation nor fibrosis was observed in a Rec2 vector harboring expression cassette without a transgene. The Rec2-no transgene vector was used as control in Cre-loxP knockdown study. Rec2-Cre injection had no significant effects on body weight (Figure 4c) while slightly decreased food intake (control: 3.36 ± 0.39 g/day; Cre: 3.02 ± 0.09 g/day; P = 0.041) during the 8 weeks of experiment. No significant changes were observed in insulin tolerance test at fed condition (Figure 4d) or glucose tolerance test at fast (Figure 4e) 4 and 5 weeks after Rec2-Cre injection, respectively. By 8 weeks after Rec2-Cre injection, no significant effects on serum biomarkers were found including insulin, leptin, glucose, cholesterol, and triglyceride (Figure 4f). However, Rec2-Cre decreased IWAT mass by more than 50% (Figure 4a–c), while had no effects on BAT or visceral WAT. Western blot showed that Rec2-Cre knocked down IR protein level by 53% (Figure 4g,h) consistent to the knockdown at mRNA level measured by quantitative RT-PCR (Figure 5b). No changes of IR expression were found in liver, skeletal muscle, or visceral WAT (data not shown). Adipocytes in Rec2-Cre–injected IWAT appeared smaller than that in control (Figure 5a). No increases of apoptosis or cell death were observed in TUNEL (TdT-mediated dUTP-biotin nick end labeling) assay or active caspase-3 immunohistochemistry (data not shown). Gene expression profiling revealed extensive molecular changes in Rec2-Cre–injected IWAT (Figure 5b). Adipokines adiponectin, leptin, and resistin expression were all suppressed. Adipogenic markers *Ap2* and *Pparg* as well as WAT marker *Hoxc9* were also decreased significantly.[13,14] Both lipogenic (*Fasn*) and lipolytic (*Cpt1a*) markers were reduced together with oxidative markers *Cytc* and *Ppargc1a*.[15,16] In addition, angiogenic markers *Cd31* and *Vegf* were also decreased.[17] In contrast, macrophage marker F4/80 and inflammatory M1 macrophage marker *Mgl1* were increased[18,19] (Figure 5b). Immunohistochemistry confirmed the increase of F4/80 in Rec2-Cre–injected IWAT. The extensive molecular changes indicated that the disruption of IR signaling in adult IWAT led to dysfunction of the transduced fat pad, although no overt systemic impact was observed in this relative short-term

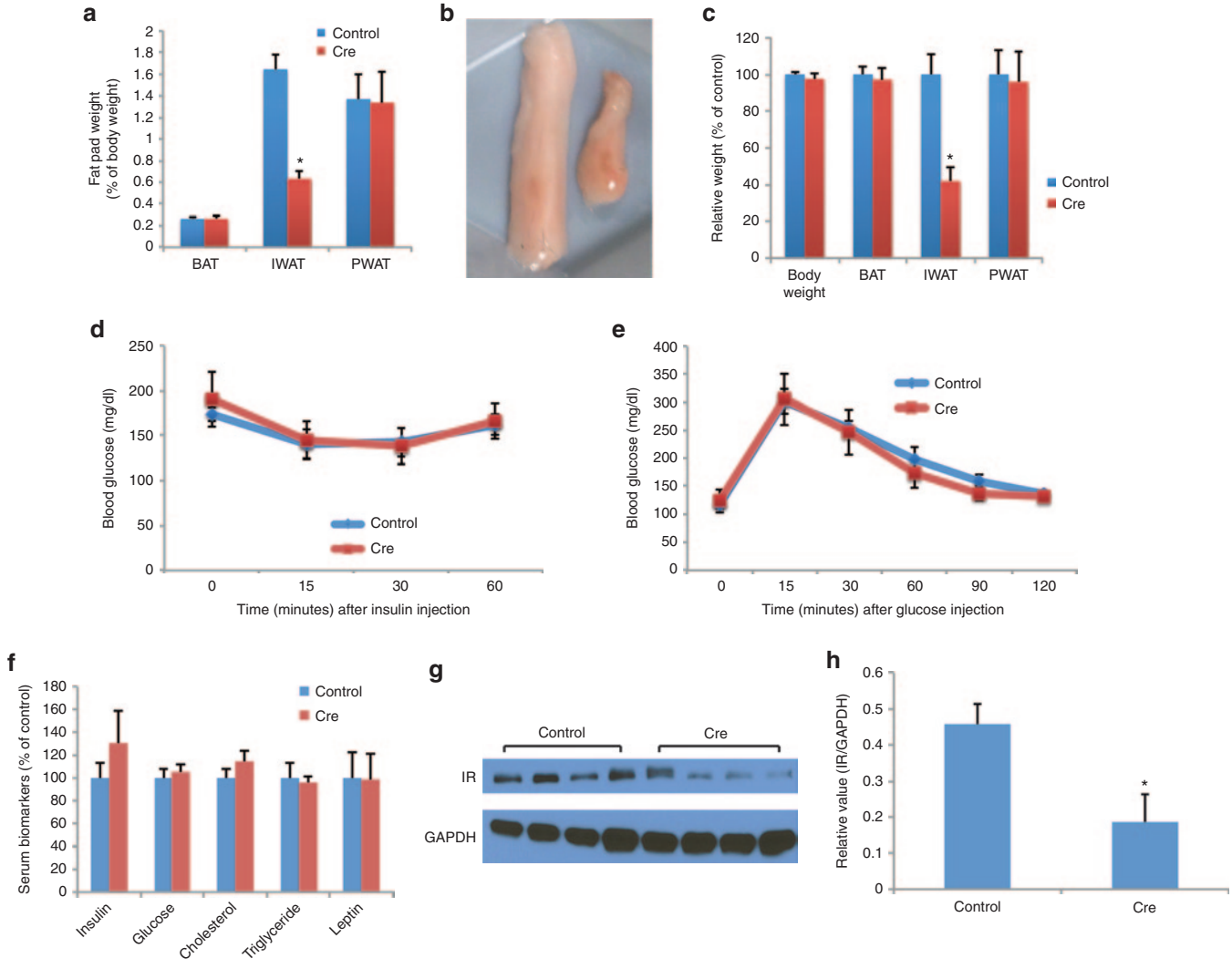

Figure 4 Rec2-Cre–mediated IR knockdown in IWAT. (**a**) Rec2-Cre decreased IWAT mass ($n = 7$ per group; $^*P < 0.05$). (**b**) Representative IWAT 8 weeks after Rec2 injection. (**c**) Fat mass calibrated to body weight ($n = 7$ per group, $^*P < 0.05$). (**d**) Insulin tolerance test ($n = 7$ per group). (**e**) Glucose tolerance ($n = 7$ per group). (**f**) Serum biomarkers ($n = 7$ per group). (**g**, **h**) Western blot of IR and quantification ($n = 4$ per group, $^*P < 0.05$). IR, insulin receptor; IWAT, inguinal white adipose tissue.

experiment. Interestingly, the hypothalamus was able to "sense" the knockdown of IR in IWAT (Figure 5c). For example, the neuronal activity marker Fos showed a trend of upregulation in the hypothalamus when IR was knocked down in IWAT.[20] Leptin receptor expression was significantly upregulated in the hypothalamus. Brain-derived neurotrophic factor (BDNF) and cocaine-amphetamine–regulated transcript (Cartpt), both anorexigenic,[21,22] were upregulated, which might underlie the decreased food intake.

Rec2-Cre knocks down IR in BAT

Rec2-Cre was injected bilaterally to BAT of male IR^{lox} mice at the age of 6 weeks (1×10^9 vg per injection) with empty Rec2 vector as control. No significant difference was found in body weight (Figure 6a) or food intake (control: 4.10 ± 0.19 g/day; Cre: 4.32 ± 0.35 g/day; $P = 0.34$). Similar to IWAT IR knockdown, no significant effects on insulin tolerance (Figure 6d) or glucose tolerance (Figure 6e) or serum biomarkers (Figure 6f) were observed. Rec2-Cre–injected BAT was 50% smaller than control vector–injected BAT (Figure 6a–c), while no difference in subcutaneous WAT or epididymal WAT mass was found (Figure 6a,c). Western blot showed ~60% decrease of IR at protein level (Figure 6g,h), while quantitative RT-PCR showed 50% downregulation at mRNA level (Figure 7b). Hematoxylin and eosin staining showed massive reduction of brown adipocytes size with far less lipid droplets (Figure 7a). Rec2-Cre–injected BAT showed marked increase of eosinophilia compared with controls (Figure 7a). These results indicate BAT lipoatrophy, although no apoptosis was found by TUNEL assay or active caspase-3 analysis (data not shown). Cre is reported to have no impact on BAT,[23] and therefore, the phenotypic changes in Rec2-Cre–injected BATs were due to the IR knockdown. The decrease of BAT mass and potential dysfunction had no effect on rectal temperature measured at room temperature (control: 36.2 ± 0.2°C; Cre: 36.8 ± 0.1°C; $P = 0.1$). Rec2-Cre injection to BAT did not change IR expression in liver or skeletal muscle (Figure 7d) while interestingly upregulated IR expression in visceral WAT (Figure 7d). In contrast to IR knockdown in IWAT (Figure 5b), Rec2-Cre led to less gene expression changes (Figure 7b), although the IR knockdown level was similar. However, greater induction of macrophage markers and inflammation markers were observed in BAT (Figure 7b) with M1 macrophage marker *Mcp1* increased by 12-fold and inflammatory marker *Saa3* increased by 18-fold.[24] The disruption of IR signaling in

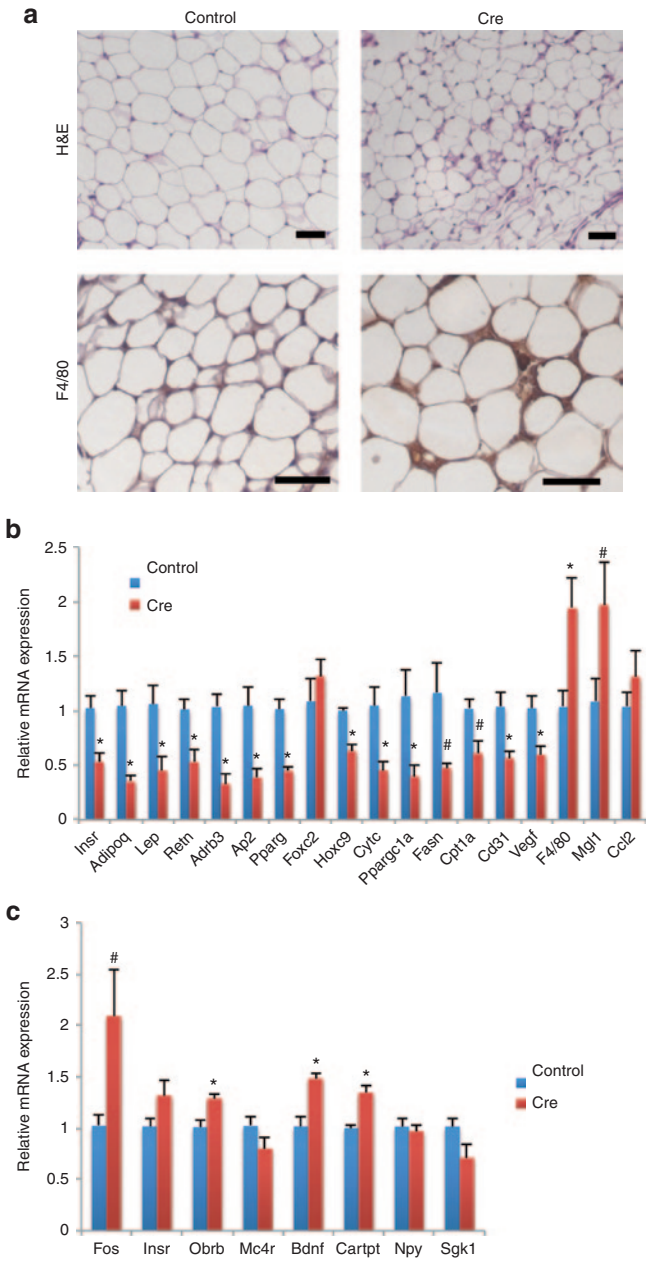

Figure 5 Phenotypic changes induced by Rec2-Cre–mediated IR knockdown in IWAT. (**a**) Hematoxylin and eosin staining and F4/80 immunohistochemistry. Scale bar = 50 µm. (**b**) Gene expression profile of Rec2-injected IWAT ($n = 7$ per group, $^{*}P < 0.05$, $^{\#}P = 0.06$). (**c**) Gene expression profile of hypothalamus ($n = 7$ per group, $^{*}P < 0.05$, $^{\#}P = 0.06$). IR, insulin receptor; IWAT, inguinal white adipose tissue.

BAT induced gene expression changes in the hypothalamus (Figure 7c) but showed a different profile compared with IR knockdown in IWAT (Figure 5c). IR expression in hypothalamus showed a trend of upregulation, while melanocortin receptor 4 (Mc4r), a critical pathway in energy balance regulation,[25] was downregulated.

DISCUSSION

A critical barrier of genetic manipulation of adipose tissue for basic research and translational studies has been the difficulties of transducing adipose tissue with viral vectors such as rAAV. Here, we demonstrate that a newly engineered nonhuman primate–derived hybrid rAAV serotype efficiently transduced both BAT and WAT when directly injected to the fat pad. Rec2 vector showed highest transduction efficacy with lowest off-target transgene expression primarily in liver. Several strategies can be employed to enhance fat-specific expression: using an adipose-specific promoter to drive transgene expression[24,26–28]; incorporating a microRNA targeting the transgene that is driven by tissue-specific promoters of the tissues intended to avoid[11]; placing a tissue-specific microRNA target into the 3′ untranslated region of a transgene to mitigate the transgene expression in unintended cells because the specific microRNA is only expressed in the unintended cells such as a liver-specific microRNA-122[29–31]; or the combination of these strategies. Fat pad injection of Rec2 vector showed minimal off-target transgene expression in both the reporter gene experiment using GFP and the functional experiment using the Cre-loxP system. However, restriction of off-target expression of transgene is necessary for systemic gene delivery. Our unpublished data showed that with intravenous infusion, Rec2 showed the greatest transduction of the target tissue cardiac muscle among multiple natural and engineered serotypes while liver also showed high transgene expression. Investigations on targeting adipose tissue via systemic administration of Rec2 are underway.

Several hundred human and nonhuman primate isolates of AAV have been discovered.[32] And the reengineered variants, chimeric, and mutant strains together with the naturally occurring serotypes yielded a broad and versatile AAV vector toolkit for both basic research and clinical application.[5] Our data show that Rec2 serotype transduces adipose tissue superior to natural serotypes tested. The Rec2 serotype was generated by capsid shuffling of AAV strains isolated from the primate brain. Future studies to isolate AAV stains directly from primate adipose tissue and then to engineer hybrid and mutant strains based on the adipose-derived natural serotypes can further improve tissue tropism and gene transfer efficiency.

As a proof-of-efficacy, we used the Rec2 vector to knockdown IR via Cre-loxP recombination in both BAT and WAT. Our data demonstrate that a low-dose injection of Rec2-Cre to fat pads of adult animal led to 50% decrease of IR level and the ensuring loss of fat mass, molecular and morphological changes consistent with impaired adipose function. Fat-specific IR knockout mouse,[33] BAT-specific IR knockout mouse,[23] and fat-specific IR and insulin-like growth factor-1 receptor double knockout mouse[34] have been generated. These knockout strains have revealed that IR signaling plays a crucial role in the control of fat development. Our data using viral vector–mediated IR knockdown in adult animal suggest that adipose IR signaling is critical to the maintenance of both BAT and WAT. Some phenotypic changes are similar to IR knockout mice. For example, Rec2-Cre injection to BAT led to loss of BAT mass by 50%, which was comparable to the BAT-specific IR knockout mice, whose IR expression in BAT was reduced by 95%.[23] The marked reduction of brown adipocyte size and lipid droplet size as well as increased eosinophilia in Rec2-Cre–injected BAT were consistent to BAT-specific IR knockout mice. BAT-specific IR knockout mice also did not show altered insulin tolerance, although progressive glucose intolerance occurred at the age of 6 months. Long-term experiment using Rec2-Cre might reveal the impact on glucose tolerance that did not change by 8 weeks after viral vector injection. Viral vector–mediated IR knockdown in adipose tissue not only helped to distinguish the role of IR in development from maintenance but also revealed a few changes that were not reported in various fat-specific IR knockout mice such as the strong induction of macrophage markers and the hypothalamic "sensing" of the disruption of IR signaling in specific fat depot. The role of macrophage and inflammation in adipose remodeling in response to IR knockdown warrants further investigation.[35] Furthermore, recent studies have demonstrated that insulin signaling can occur locally and therefore

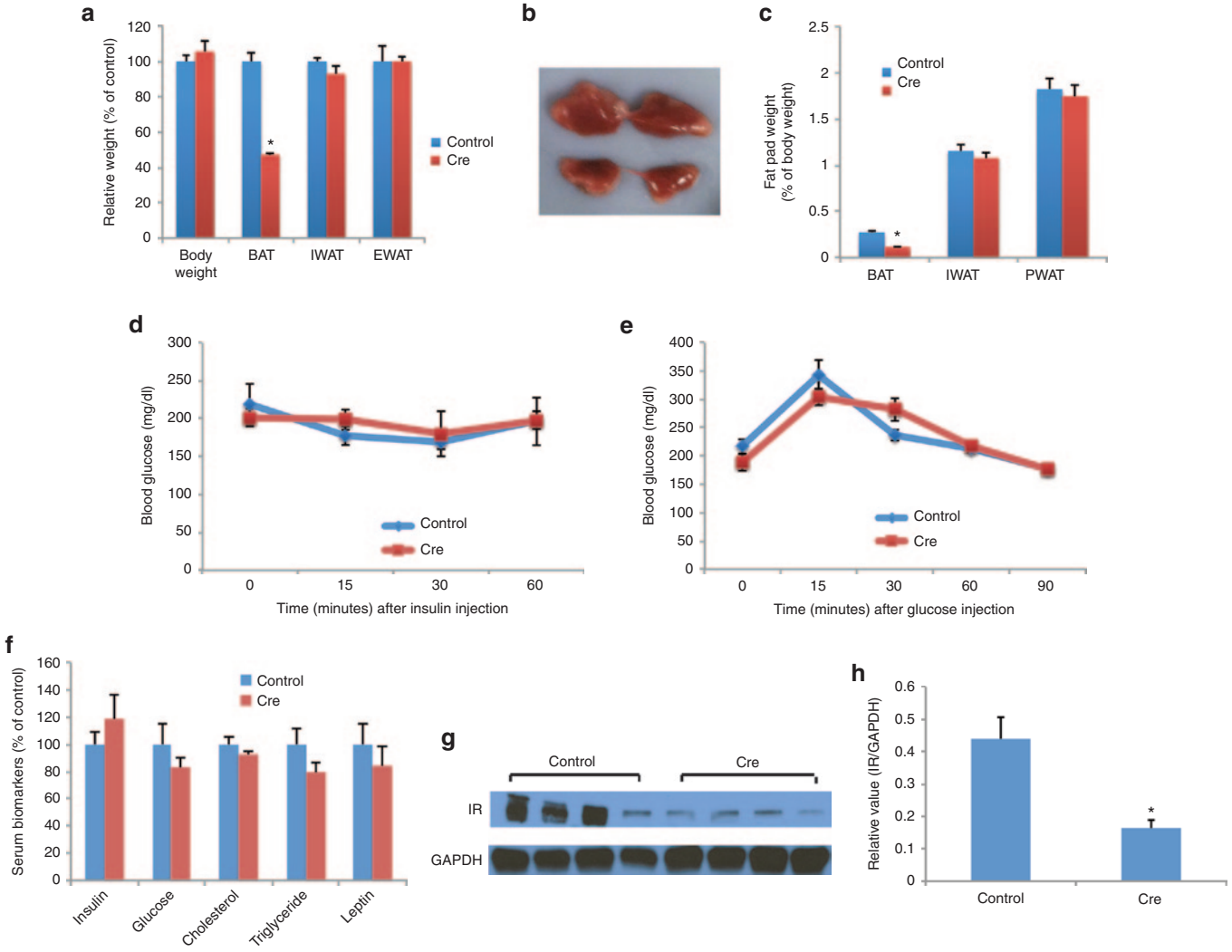

Figure 6 Rec2-Cre–mediated IR knockdown in BAT. (**a**) Rec2-Cre decreased BAT mass ($n = 6$ per group, $^*P < 0.05$). (**b**) Representative BAT 8 weeks after Rec2 injection. (**c**) Fat mass calibrated to body weight ($n = 6$ per group, $^*P < 0.05$). (**d**) Insulin tolerance test ($n = 6$ per group). (**e**) Glucose tolerance ($n = 6$ per group). (**f**) Serum biomarkers ($n = 6$ per group). (**g**, **h**) Western blot of IR and quantification ($n = 4$ per group, $^*P < 0.05$). BAT, brown adipose tissue; GAPDH, glyceraldehyde-3-phosphate dehydrogenase.

allow tissue-specific responses to challenges.[36] Emerging evidence suggests that local insulin signaling, rather than systemic insulin signaling, plays a critical role in regulating stem cell behavior.[37,38] Given the drastic decrease of fat pad mass when adipose IR was knocked down by 50%, Rec2 vector can serve as a powerful tool to further study the role of local insulin signaling in adipose stem cell behavior. The changes in gene expression profile of hypothalamus suggest that the adaptive responses in nontargeted fat depots as well as systemic changes are likely modulated via central mechanisms. It has been increasingly recognized that various fat depots are developmentally, genetically, and functionally distinguishable. Furthermore, adipose tissue responds to environmental, metabolic, and other challenges in a depot-specific manner.[39] Therefore, the Rec2 vector provides a tool to study depot-specific function and modulation, and the interaction among various fat depots, organs, and the CNS.

In this study, we used a knockdown approach to demonstrate the application of adipose-targeting viral vectors. This technology provides other capabilities, for example, allows genetic manipulation of adipose tissue to induce phenotypic changes of transduced adipose tissue or supply a transgene product into the systemic circulation for gene therapy. We reported that AAV-mediated brain-derived neurotrophic factor overexpression in the hypothalamus decreased adiposity, induced brown adipocyte-like cells in WAT, enhanced energy expenditure, and inhibited peripheral tumor progression.[12,40] Molecular therapy directly targeting the adipose tissue would be an attractive alternative to neurosurgical approaches with advantages including easy access to the targeting tissues, potentially enhanced tissue specificity, and safe removal in case that therapeutic gene expression is no longer required. Studies on the efficacy of Rec2-mediated delivery of genes that induce browning such as PGC1-α[15] and UCP1[41] to WAT in a disease model are being carried out in our laboratory.

In summary, our data demonstrate that a novel engineered primate-derived AAV serotype Rec2 efficiently transduce both BAT and WAT. One administration of Rec2-Cre led to sufficient knockdown of IR in adipose tissue of adult animal with some phenotypic changes similar to fat-specific IR knockout mice while others previously not revealed in knockout mice. Further development and refinement of AAV vectors targeting adipose tissue will provide tools to study adipose function and regulation as well as to facilitate therapeutic applications.

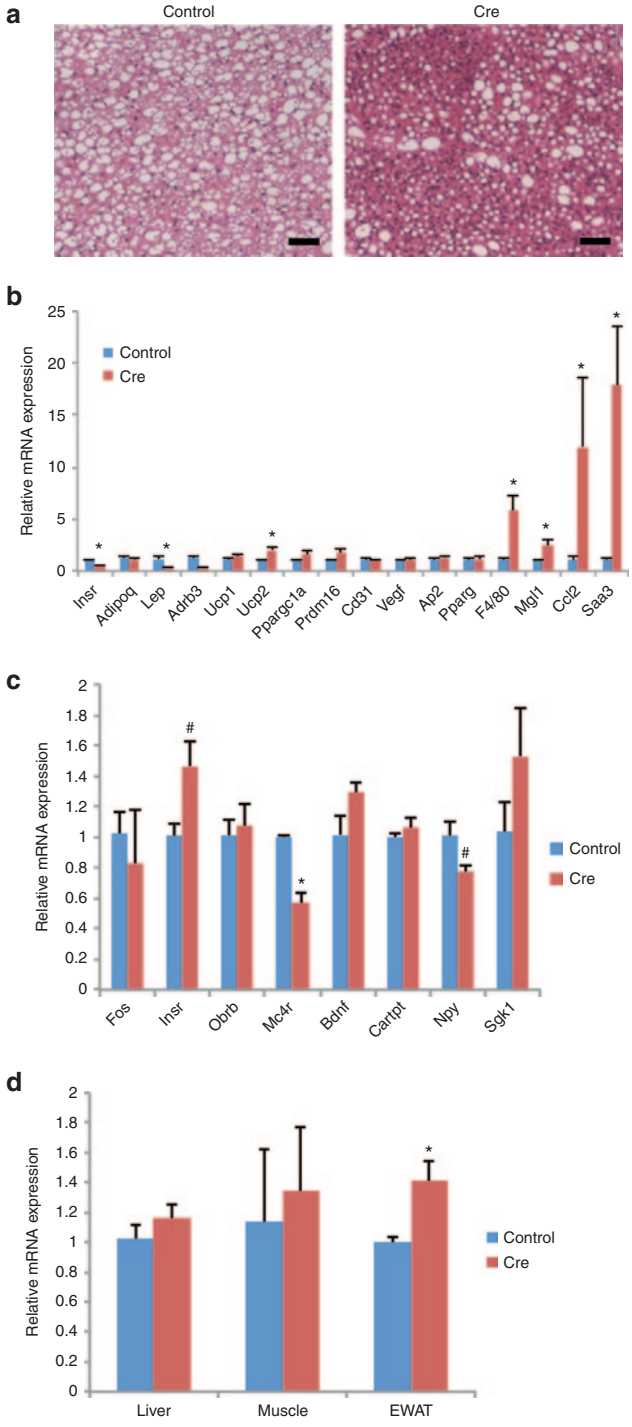

Figure 7 Phenotypic changes induced by Rec2-Cre–mediated IR knockdown in BAT. (**a**) Hematoxylin and eosin staining of Rec2-injected BAT. Scale bar = 50 µm. (**b**) Gene expression profile of Rec2-injected BAT ($n = 6$ per group, $^*P < 0.05$). (**c**) Gene expression profile of hypothalamus ($n = 6$ per group, $^*P < 0.05$, $^\#P = 0.06$). (**d**) Insulin receptor expression in liver, muscle, and visceral WAT ($n = 6$ per group, $^*P < 0.05$). BAT, brown adipose tissue; IR, insulin receptor.

MATERIALS AND METHODS

AAV vectors

The recombinant AAV capsid serotypes (Rec1–4) were generated by shuffling the fragments of capsid sequences that matched in all three nonhuman primate AAV seroptyes (cy5, rh20, and rh39) and AAV8. The three new recombinant serotypes previously identified, with greater transduction efficiency than rAAV8, cy5, rh20, and rh39, were originally supplied by Guangping Gao and the Gene Therapy Program Vector Core, Department of Medicine, University of Pennsylvania, where further details of the identification of these sequences are available. The details of Rec1–4 serotypes are described before.[8] To generate hybrid AAV vectors, GFP was cloned into an AAV expression plasmid under the control of the CBA (hybrid cytomegalovirus–chicken β-actin) promoter and containing woodchuck hepatitis virus posttranscriptional regulatory element (WPRE) and bovine growth hormone polyadenylation signal flanked by AAV2-inverted terminal repeats. Human embryonic kidney 293 cells were cotransfected with three plasmids—AAV plasmid, appropriate helper plasmid encoding rep and cap (Rec1–4) genes or AAV1, AAV8, AAV9, and adenoviral helper pF Δ6—using standard $CaPO_4$ transfection. rAAV vectors were purified from the cell lysate by ultracentrifugation through an iodixanol density gradient. Vectors were titered using quantitative PCR (ABI Prism 7700; Applied Biosystems, Foster City, CA). Finally, the rAAV2/Rec vectors were assayed using standard *in vivo* protocols comparing transduction efficiency to rAAV2/8. With intravenous infusion, rAAV2/Rec2 showed the greatest transduction of the target tissue (cardiac muscle), and with direct intracerebral administration, rAAV2/Rec3 led to the greatest neuronal cell transduction (manuscript in preparation). Rec2 vector expressing Cre under the control of CBA promoter was generated similar to GFP vectors.

Mice

Wild-type C57BL/6 mice were purchased from Charles River (Spencerville, OH). Homozygous IR^{lox} mice were purchased from Jackson Laboratory (Bar Harbor, ME) (B6.129S4(FVB)-$Insr^{tm1Khn/J}$). We carried out all mice experiments in compliance with the regulations of the Institutional Animal Ethics Committees of the Ohio State University.

rAAV injection to inguinal WAT

Animals aged 6 weeks were anesthetized using 2% isoflurane in O_2. Once anesthesia was fully induced, the animal was shaved with a hair trimmer in the area where the IWAT was located. The shaved area was sterilized with three alternating wipes of Betadine and 70% ethanol. The animal was laid flat on its stomach, and an incision was made roughly 1.5 cm lateral to the spinal cord, slightly above the hind legs. The IWAT was immediately visible to the naked eye if the incision was made in the correct location. Forceps and surgical scissors were used to cut any connective tissue to the skin, and the adipose tissue was grabbed firmly with the forceps. The adipose tissue was held in place with the forceps, and the rAAV was injected (1.0×10^{10} vg per 20 µl in phosphate-buffered saline) with a 0.3 cc, 31 G insulin syringe. The tissue was lifted to ensure no virus leaked during injection. The fat pad was gently forced back into the body cavity, and the wound was closed with a 4-0 PDS II FS-2 suture. The closed surgical wound was coated with Betadine for sanitary purposes. The procedure was repeated on the opposite IWAT to complete the bilateral injection.

rAAV injection to retroperitoneal WAT

Animals aged 6 weeks were given a ketamine/xylazine cocktail (87/13 mg/kg i.p., 250 µl) for anesthesia. Once anesthesia was fully induced, the animal's lower back was shaved using a hair trimmer, and the shaved area was sterilized with three alternating wipes of Betadine and 70% ethanol. A small incision was made ~1.0 cm lateral from the spinal cord above the expected location of the desired adipose tissue. The muscle was opened using surgical scissors to reveal the adipose tissue. Forceps were used to move the fat pad into a position where the kidney could be visualized in order to confirm that the correct fat pad was located. Once confirmation was obtained, the adipose tissue was held in place with the forceps, and 50 µl of virus was injected with a 0.3 cc, 31 G insulin syringe. The tissue was lifted to ensure that no virus leaked during injection. The fat pad was gently forced back into the cavity, and the muscle was closed with a 6-0 polypropylene P-13 suture, followed by the closure of the skin flap by a 4-0 PDS II FS-2 suture. The closed surgical wound was coated with betadine for sanitary purposes.

rAAV injection to interscapular BAT

Animals aged 6 weeks were anesthetized using 2% isoflurane in O_2. Once anesthesia was fully induced, the animal was shaved with a hair trimmer bilateral to the spinal cord, roughly 1 cm below the head. The shaved area was sterilized with three alternating wipes of Betadine and 70% ethanol. The animal

was laid flat on its stomach, and a shallow incision was made in the center of the shaved area and extended ~0.5 cm bilateral. Another small incision was made to cut through the thin layer of WAT to reveal the BAT. Forceps were used to firmly grasp the distinct BAT, and the desired rAAV was injected (1.0×10^9 vg per 20 µl) with a 0.3 cc, 31 G insulin syringe. The tissue was lifted to ensure that no virus leaked during injection. The procedure was repeated on the opposite side to complete the bilateral injection. The fat pad was gently forced back into the body cavity, and the wound was closed with a 4-0 PDS II FS-2 suture. The closed surgical wound was coated with Betadine for sanitary purposes.

Glucose tolerance test

We injected mice intraperitoneally with glucose solution (1 mg glucose per kg body weight) after an overnight fast. We obtained blood from the tail at various time points. We measured blood glucose concentrations with a portable glucose meter (ReliOn Ultima; Abbott Diabetes Care, Alameda, CA).

Insulin tolerance test

We injected mice intraperitoneally with insulin (0.75 unit per kg body weight) at 2 PM without a fast. We obtained blood from the tail and measured the blood glucose concentration as described above.

Serum harvest and biomarkers measurement

Blood was collected following decapitation. We prepared serum by allowing the blood to clot for 30 minutes on ice followed by centrifugation. Serum was at least diluted 1:5 in serum assay diluent and assayed using the DuoSet ELISA Development System (R&D Systems, Minneapolis, MN) for mouse Leptin. Insulin was measured using Mercodia ultrasensitive mouse insulin ELISA (ALPCO Diagnostics, Salem, NH). Glucose was measured using QuantiChrom Glucose Assay (BioAssay Systems, Hayward, CA). Total cholesterol was measured using Cholesterol E test kit (Wako Diagnostics, Richmond, VA).

Body weight and food consumption

We maintained the mice on a normal 12 h/12 h light/dark cycle with access to food and water *ad libitum* throughout the experiment. Body weight of individual mouse was recorded twice weekly. Food consumption was recorded twice weekly as the total food consumption and represented as the average of food consumption per mouse per day.

Quantitative RT-PCR

We dissected BAT and WAT and hypothalamus and isolated total RNA using RNeasy Lipid Kit plus RNase-free DNase treatment (Qiagen, Hilden, Germany). We generated first-strand cDNA using TaqMan Reverse Transcription Reagent (Applied Biosystems) and carried out quantitative PCR using Light Cycler (Roche) with the Power SYBR Green PCR Master Mix (Applied Biosystems). We designed primers to detect the following mouse mRNA: *Fos*, *Cartp*, *Npy*, *Mc4r*, *Sgk1*, *Insr*, *Lepr*, *Bdnf*, *Ucp1*, *Ucp2*, *Lep*, *Adipoq*, *Ap2*, *Pparg*, *Fasn*, *Ap2*, *Resn*, *Prdm16*, *Hoxc9*, *Cytc*, *Cpt1a*, *Cd31*, *Vegf*, *F4/80*, *Mgl1*, *Ccl2*, *Foxc2*, *Ppargc1a*, *Saa3*, and *Adrb3*. Primer sequences are available on request. We calibrated data to endogenous control *Actb* or *Hprt1* and quantified the relative gene expression using the equation $T_0/R_0 = \mathrm{K} \times 2^{(\mathrm{CT,R} - \mathrm{CT,T})}$. T_0 is the initial number of target gene mRNA copies, R_0 is the initial number of internal control gene mRNA copies, CT,T is the threshold cycle of the target gene, CT,R is the threshold cycle of the internal control gene, and K is a constant.

Immunohistochemistry

We cut paraffin-embedded sections (4 µm) of adipose tissues and subjected the sections to citrate-based antigen retrieval followed by incubations with antibody against F4/80 (Serotec) or GFP (Abcam). The sections were visualized with DAB and counterstained with hematoxylin or Cy2-conjugated secondary antibody for immunofluorescence.

Western blot

We used ALLPrep DNA/RNA mini kit (Qiagen) to simultaneously purify genomic DNA and total RNA. Proteins were precipitated from the flow-through using acetone according to the manufacturer's protocol. Rabbit anti-GFP (Abcam; 1:400), rabbit anti-IR (Santa Cruz; 1:1,000), and rabbit anti–glyceraldehyde-3-phosphate dehydrogenase (Abcam; 1:1,000) were used in western blot analysis. Image J software was used to quantify western blot data.

Statistical analysis

Values are expressed as mean ± SEM. We used JMP software to analyze the following: (i) two-way analysis of variance for food intake, insulin tolerance, and glucose tolerance and (ii) one-way analysis of variance for serum biomarker measurements, body weight and adipose tissue weight, body temperature, quantitative RT-PCR data, and western blot quantification.

CONFLICT OF INTEREST

The authors declare no conflict of interest.

ACKNOWLEDGMENTS

This work was supported by NIH grants CA163640, CA166590, CA178227, and AG041250 (to L.C.) and NS44576 (to M.D.).

REFERENCES

1 Spiegelman, BM and Enerbäck, S (2006). "The adipocyte: a multifunctional cell". *Cell Metab* **4**: 425–427.
2 Nagamatsu, S, Nakamichi, Y, Ohara-Imaizumi, M, Ozawa, S, Katahira, H, Watanabe, T *et al*. (2001). Adenovirus-mediated preproinsulin gene transfer into adipose tissues ameliorates hyperglycemia in obese diabetic KKA(y) mice. *FEBS Lett* **509**: 106–110.
3 Morizono, K, De Ugarte, DA, Zhu, M, Zuk, P, Elbarbary, A, Ashjian, P *et al*. (2003). Multilineage cells from adipose tissue as gene delivery vehicles. *Hum Gene Ther* **14**: 59–66.
4 Mingozzi, F and High, KA (2011). Therapeutic *in vivo* gene transfer for genetic disease using AAV: progress and challenges. *Nat Rev Genet* **12**: 341–355.
5 Asokan, A, Schaffer, DV and Samulski, RJ (2012). The AAV vector toolkit: poised at the clinical crossroads. *Mol Ther* **20**: 699–708.
6 Mizukami, H, Mimuro, J, Ogura, T, Okada, T, Urabe, M, Kume, A *et al*. (2006). Adipose tissue as a novel target for *in vivo* gene transfer by adeno-associated viral vectors. *Hum Gene Ther* **17**: 921–928.
7 Zhang, FL, Jia, SQ, Zheng, SP and Ding, W (2011). Celastrol enhances AAV1-mediated gene expression in mice adipose tissues. *Gene Ther* **18**: 128–134.
8 Charbel Issa, P, De Silva, SR, Lipinski, DM, Singh, MS, Mouravlev, A, You, Q *et al*. (2013). Assessment of tropism and effectiveness of new primate-derived hybrid recombinant AAV serotypes in the mouse and primate retina. *PLoS ONE* **8**: e60361.
9 Gao, G, Vandenberghe, LH, Alvira, MR, Lu, Y, Calcedo, R, Zhou, X *et al*. (2004). Clades of adeno-associated viruses are widely disseminated in human tissues. *J Virol* **78**: 6381–6388.
10 Lawlor, PA, Bland, RJ, Mouravlev, A, Young, D and During, MJ (2009). Efficient gene delivery and selective transduction of glial cells in the mammalian brain by AAV serotypes isolated from nonhuman primates. *Mol Ther* **17**: 1692–1702.
11 Cao, L, Lin, EJ, Cahill, MC, Wang, C, Liu, X and During, MJ (2009). Molecular therapy of obesity and diabetes by a physiological autoregulatory approach. *Nat Med* **15**: 447–454.
12 Cao, L, Liu, X, Lin, EJ, Wang, C, Choi, EY, Riban, V *et al*. (2010). Environmental and genetic activation of a brain-adipocyte BDNF/leptin axis causes cancer remission and inhibition. *Cell* **142**: 52–64.
13 Kajimura, S, Seale, P, Tomaru, T, Erdjument-Bromage, H, Cooper, MP, Ruas, JL *et al*. (2008). Regulation of the brown and white fat gene programs through a PRDM16/CtBP transcriptional complex. *Genes Dev* **22**: 1397–1409.
14 Petrovic, N, Walden, TB, Shabalina, IG, Timmons, JA, Cannon, B and Nedergaard, J (2010). Chronic peroxisome proliferator-activated receptor gamma (PPARgamma) activation of epididymally derived white adipocyte cultures reveals a population of thermogenically competent, UCP1-containing adipocytes molecularly distinct from classic brown adipocytes. *J Biol Chem* **285**: 7153–7164.
15 Tiraby, C, Tavernier, G, Lefort, C, Larrouy, D, Bouillaud, F, Ricquier, D *et al*. (2003). Acquirement of brown fat cell features by human white adipocytes. *J Biol Chem* **278**: 33370–33376.
16 Puigserver, P, Wu, Z, Park, CW, Graves, R, Wright, M and Spiegelman, BM (1998). A cold-inducible coactivator of nuclear receptors linked to adaptive thermogenesis. *Cell* **92**: 829–839.
17 Zhang, QX, Magovern, CJ, Mack, CA, Budenbender, KT, Ko, W and Rosengart, TK (1997). Vascular endothelial growth factor is the major angiogenic factor in omentum: mechanism of the omentum-mediated angiogenesis. *J Surg Res* **67**: 147–154.
18 Barbatelli, G, Murano, I, Madsen, L, Hao, Q, Jimenez, M, Kristiansen, K *et al*. (2010). The emergence of cold-induced brown adipocytes in mouse white fat depots is determined predominantly by white to brown adipocyte transdifferentiation. *Am J Physiol Endocrinol Metab* **298**: E1244–E1253.
19 Thompson, RJ, Doran, JF, Jackson, P, Dhillon, AP and Rode, J (1983). PGP 9.5–a new marker for vertebrate neurons and neuroendocrine cells. *Brain Res* **278**: 224–228.

20 Nedivi, E, Hevroni, D, Naot, D, Israeli, D and Citri, Y (1993). Numerous candidate plasticity-related genes revealed by differential cDNA cloning. *Nature* **363**: 718–722.
21 Rios, M, Fan, G, Fekete, C, Kelly, J, Bates, B, Kuehn, R *et al*. (2001). Conditional deletion of brain-derived neurotrophic factor in the postnatal brain leads to obesity and hyperactivity. *Mol Endocrinol* **15**: 1748–1757.
22 Xu, B, Goulding, EH, Zang, K, Cepoi, D, Cone, RD, Jones, KR *et al*. (2003). Brain-derived neurotrophic factor regulates energy balance downstream of melanocortin-4 receptor. *Nat Neurosci* **6**: 736–742.
23 Guerra, C, Navarro, P, Valverde, AM, Arribas, M, Brüning, J, Kozak, LP *et al*. (2001). Brown adipose tissue-specific insulin receptor knockout shows diabetic phenotype without insulin resistance. *J Clin Invest* **108**: 1205–1213.
24 Sun, K, Wernstedt Asterholm, I, Kusminski, CM, Bueno, AC, Wang, ZV, Pollard, JW *et al*. (2012). Dichotomous effects of VEGF-A on adipose tissue dysfunction. *Proc Natl Acad Sci USA* **109**: 5874–5879.
25 Flier, JS (2004). Obesity wars: molecular progress confronts an expanding epidemic. *Cell* **116**: 337–350.
26 He, W, Barak, Y, Hevener, A, Olson, P, Liao, D, Le, J *et al*. (2003). Adipose-specific peroxisome proliferator-activated receptor gamma knockout causes insulin resistance in fat and liver but not in muscle. *Proc Natl Acad Sci USA* **100**: 15712–15717.
27 Pajvani, UB, Trujillo, ME, Combs, TP, Iyengar, P, Jelicks, L, Roth, KA *et al*. (2005). Fat apoptosis through targeted activation of caspase 8: a new mouse model of inducible and reversible lipoatrophy. *Nat Med* **11**: 797–803.
28 Segawa, K, Matsuda, M, Fukuhara, A, Morita, K, Okuno, Y, Komuro, R *et al*. (2009). Identification of a novel distal enhancer in human adiponectin gene. *J Endocrinol* **200**: 107–116.
29 Brown, BD, Venneri, MA, Zingale, A, Sergi Sergi, L and Naldini, L (2006). Endogenous microRNA regulation suppresses transgene expression in hematopoietic lineages and enables stable gene transfer. *Nat Med* **12**: 585–591.
30 Geisler, A, Jungmann, A, Kurreck, J, Poller, W, Katus, HA, Vetter, R *et al*. (2011). microRNA122-regulated transgene expression increases specificity of cardiac gene transfer upon intravenous delivery of AAV9 vectors. *Gene Ther* **18**: 199–209.
31 Qiao, C, Yuan, Z, Li, J, He, B, Zheng, H, Mayer, C *et al*. (2011). Liver-specific microRNA-122 target sequences incorporated in AAV vectors efficiently inhibits transgene expression in the liver. *Gene Ther* **18**: 403–410.
32 Gao, G, Vandenberghe, LH and Wilson, JM (2005). New recombinant serotypes of AAV vectors. *Curr Gene Ther* **5**: 285–297.
33 Blüher, M, Michael, MD, Peroni, OD, Ueki, K, Carter, N, Kahn, BB *et al*. (2002). Adipose tissue selective insulin receptor knockout protects against obesity and obesity-related glucose intolerance. *Dev Cell* **3**: 25–38.
34 Boucher, J, Mori, MA, Lee, KY, Smyth, G, Liew, CW, Macotela, Y *et al*. (2012). Impaired thermogenesis and adipose tissue development in mice with fat-specific disruption of insulin and IGF-1 signalling. *Nat Commun* **3**: 902.
35 Sun, K, Kusminski, CM and Scherer, PE (2011). Adipose tissue remodeling and obesity. *J Clin Invest* **121**: 2094–2101.
36 Cheetham, SW and Brand, AH (2013). Cell biology. Insulin finds its niche. *Science* **340**: 817–818.
37 Chell, JM and Brand, AH (2010). Nutrition-responsive glia control exit of neural stem cells from quiescence. *Cell* **143**: 1161–1173.
38 Sousa-Nunes, R, Yee, LL and Gould, AP (2011). Fat cells reactivate quiescent neuroblasts via TOR and glial insulin relays in Drosophila. *Nature* **471**: 508–512.
39 Cinti, S (2012). The adipose organ at a glance. *Dis Model Mech* **5**: 588–594.
40 Cao, L, Choi, EY, Liu, X, Martin, A, Wang, C, Xu, X *et al*. (2011). White to brown fat phenotypic switch induced by genetic and environmental activation of a hypothalamic-adipocyte axis. *Cell Metab* **14**: 324–338.
41 Nicholls, DG and Locke, RM (1984). Thermogenic mechanisms in brown fat. *Physiol Rev* **64**: 1–64.